Manuscript Information

Journal name: Clinical pharmacokinetics
NIHMS ID: NIHMS879612
Manuscript Title: In Silico Dose Prediction for Long-Acting Rilpivirine and Cabotegravir Administration to Children and Adolescents
Submitter: Springer Publishing (Sonal.shukla@springer.com, nihfunding@springer.com)

Manuscript Files

Type	Fig/Table #	Filename	Size	Uploaded
manuscript		40262_2017_557_ReferencePDF.pdf	19 pdf 98	2017-05-25 14:30:40
supplement	40262_2017_557_MOESM1_ESM.pdf	40262_2017_557_MOESM1_ESM.pdf	53 pdf 32	2017-05-25 14:30:38

This PDF receipt will only be used as the basis for generating PubMed Central (PMC) documents. PMC documents will be made available for review after conversion. Any corrections that need to be made will be done at that time. No materials will be released to PMC without the approval of an author. Only the PMC documents will appear on PubMed Central -- this PDF Receipt will not appear on PubMed Central.

In silico dose prediction for long-acting rilpivirine and cabotegravir administration to children and adolescents

Rajith KR Rajoli[1], David J Back[1], Steve Rannard[2], Caren Freel Meyers[3], Charles Flexner[4], Andrew Owen[1], Marco Siccardi[1]

[1]Department of Molecular and Clinical Pharmacology, University of Liverpool, Liverpool, UK

[2]Department of Chemistry, University of Liverpool, Crown Street, Liverpool, UK

[3]Department of Pharmacology and Molecular Sciences, Johns Hopkins School of Medicine, Baltimore, MD, USA

[4]Johns Hopkins University School of Medicine and Bloomberg School of Public Health, Baltimore, MD, USA

Author for correspondence: Dr Marco Siccardi, Department of Molecular and Clinical Pharmacology, University of Liverpool, 70 Pembroke Place, Liverpool, L69 3GF, U.K.

Tel No +44 (0) 151 794 8211

Fax No + 44 (0) 151 794 5656

E-mail: siccardi@liverpool.ac.uk

Acknowledgements:

-

Source of Funding:

This work was supported by the National Institutes of Health (R24 AI 118397).

Abstract

Background and Objectives: Long-acting injectable (LAI) antiretrovirals (ARVs) represent a pharmacological alternative to oral formulations and an innovative clinical option to address adherence and reduce drug costs. Clinical studies in children and adolescents are characterised by ethical and logistic barriers complicating the identification of dose optimisation. Physiologically-based pharmacokinetic (PBPK) modelling represents a valuable tool to inform dose finding prior to clinical trials. The objective of this study was to simulate potential dosing strategies for existing LAI depot formulations of cabotegravir and rilpivirine in children and adolescents (3-18 years) using PBPK modelling.

Methods: Whole-body PBPK models were developed to represent the anatomical, physiological, molecular processes and age related changes in children and adolescents through allometric equations. Models were validated for LAI intramuscular (IM) cabotegravir and rilpivirine in adults. Subsequently, the anatomy and physiology of children and adolescents was validated against available literature. The optimal doses of monthly administration of cabotegravir and rilpivirine were identified in children and adolescents, in order to achieve trough concentrations over the target concentrations derived in a recent efficacy trial of the same formulations.

Results: Pharmacokinetic data generated through the PBPK simulations were similar to observed clinical data in adults. Optimal doses of LAI ARVs cabotegravir and rilpivirine were predicted using the release rate observed for existing clinical formulations, for different weight groups of children and adolescents. The IM loading dose and maintenance dose of cabotegravir ranged from 200 – 600 mg and 100 – 250 mg respectively and for rilpivirine it ranged from 250 – 550 mg and 150 – 500 mg respectively across various weight groups of children ranging from 15-70 kg.

Conclusions: The reported findings represent a rational platform for the identification of suitable dosing strategies and can inform prospective clinical investigation of LAI formulations in children and adolescents.

Key Points

- Mathematical models defining anatomical, physiological and molecular processes were constructed to simulate drug pharmacokinetics in children and adolescents.
- Two clinically available long-acting formulations of cabotegravir and rilpivirine were utilised to report minimum doses needed in paediatric individuals relative to their weight.
- Evaluation of a mathematical model to identify minimum doses in children and adolescents represents an innovative method to inform dosing strategies in various kinds of population over a range of therapeutic areas.

1. Introduction

HIV (Human Immunodeficiency Virus) is one of the leading causes of death that is treated as a global priority. Initiation of HAART (Highly Active AntiRetroviral Therapy) has saved millions of lives in the past decade [1]. However, adherence to antiretroviral therapy continues to be one of the major issues hindering treatment efficacy and suboptimal adherence can extremely vary in patients ranging from 50 to 70 % in the clinical setting [2]. Currently available formulations necessitate lifelong, daily dosing and poor adherence has been attributed to numerous factors including pill fatigue, side effects and a range of socioeconomic considerations associated with different populations [3]. Problems can be particularly exacerbated in specific sub-populations of patients such as paediatric patients, where drug administration is additionally influenced by the caregiver, the family or the social environment [4].

Long acting injectable (LAI) formulations have the potential of solving the adherence issues related to oral formulations, reducing the amount of antiretroviral (ARV) used for the therapy and consequently the cost of therapy. The use of LAI formulations in paediatric patients has already been hypothesised in different disease areas and the use of LAI antipsychotics has been recently described in adolescents [5-7].

Two LAI ARV formulations have recently been developed and several others are currently under investigation [1]. Rilpivirine and cabotegravir, due to long half-life and potency, have been selected for monthly and quarterly LA administration, respectively [1, 8]. Clinical studies investigating the combination of cabotegravir and rilpivirine LAI formulations are currently ongoing to assess its safety and efficacy in adults [9]. Recent clinical trials (LATTE and LATTE-2) conducted in HIV infected adults show that cabotegravir and rilpivirine combination are safe and efficacious which provide similar antiviral activity as efavirenz plus NRTIs – tenofovir and emtricitabine [10]. The combination of rilpivirine and cabotegravir has the potential of being the first long-acting antiretroviral regimen that will not require daily oral dose of any companion drugs, representing a pivotal achievement in the antiretroviral pharmacology. However, the identification of safe and effective dosing strategies for paediatric patients is complicated by multiple factors. Differences in anatomical and physiological characteristics of children and adolescents compared to adults have a relevant effect on ADME processes and are not correctly captured through traditional allometric scaling approaches [11]. Additionally, logistic and ethical challenges in designing dose finding/optimisation studies have limited medical guidance [12].

Physiologically based pharmacokinetic (PBPK) modelling represents a valuable tool to optimise doses prior to clinical trials in paediatric patients thus minimising the time and cost invested in optimising doses. PBPK modelling is the mathematical description of anatomical, physiological and molecular processes defining pharmacokinetics. Compared to techniques usually used to select paediatric doses of adult formulations [13-16], PBPK modelling is a bottom up approach which integrates *in vitro* data such as apparent intestinal permeability, intrinsic clearance, protein binding, etc. in a mathematical description of ADME to predict *in vivo* pharmacokinetics [17].

Previous studies identified trough concentration of 1.2 µg/ml and 17 ng/ml for cabotegravir and rilpivirine respectively need to be achieved to warrant efficacy [18, 19]. No toxicity limited concentrations has been reported previously [1]. Therefore, the aim of this study was to simulate pharmacokinetics and inform optimal doses of LAI intramuscular (IM) formulations of cabotegravir and rilpivirine in at 95 % of children and adolescents aged 3 to 18 years through PBPK modelling for HIV treatment.

2. Methods

The PBPK models were constructed using Simbiology® v.4.3.1, a product of Matlab® v.8.2 (MathWorks, Natick, MA, USA 2013). Instant and uniform distribution of drugs into tissues, no reabsorption of the drug from the large intestine and a blood-flow limited model [20] were assumed. A previously published adult IM PBPK model was used in this study [21]. Cabotegravir and rilpivirine LAI IM pharmacokinetics were simulated and validated in adult PBPK models and later optimised for different weight categories of children (3-12 years) and adolescents (12-18 years). Children and adolescents between the ages 3-18 years were divided into WHO weight groups [22] and 100 virtual individuals were generated in each weight category.

2.1 Anatomy

Adult PBPK models were defined by key characteristics such as age and weight of the individual. These defining characteristic values were further used for the computation of organ and tissue volumes, as well as blood flow rates through allometric equations described by Bosgra et al. [23]. The anatomy and physiology of children and adolescents were obtained from various literature sources, validated against available clinical data prior to dose optimisation [23-33]. To improve the confidence of the constructed paediatric PBPK models, validation against intravenous lorazepam and intramuscular ceforanide as reference drugs was also conducted [34]. The various equations used for the construction of paediatric PBPK models and validation across different ages are available in Online Resource 1.

2.2 Simulation of ADME processes

Drug diffusion from the IM compartment was assumed to obey first order rate kinetics and the equation was obtained from Tegenge et al.[35]. The release rate of cabotegravir was obtained from the literature [36] and for rilpivirine, was derived using 48-week clinical data from LATTE-2, a recent Phase 2 efficacy trial of these two formulations used in combination [19]. The intrinsic clearance values derived from *in vitro* data were obtained from the literature [37] and extrapolated to systemic clearance [38]. The distribution of drug to different organs and tissues was simulated using previously published equations [21].

2.3 Model validation

The physicochemical properties of cabotegravir and rilpivirine used in the model are presented in Table 1. The validation of the drug properties against clinical data was conducted in 100 virtual adults for a 800 mg quarterly dose of cabotegravir (from weeks 12-28) and for a subsequent monthly dose of 900 mg rilpivirine (after the

initial dose of 1200 mg) [1]. The release rate of rilpivirine was identified from the clinical data using the PBPK model [1]. The release rate was also validated against the LATTE-2 pharmacokinetic curve of cabotegravir and rilpivirine. The cabotegravir release rate was assumed to be $4.54 \times 10^{-4}\,h^{-1}$ to be same as in LATTE-2 (or prior adult studies); however there was a decrease in the release rate of rilpivirine from 9×10^{-4} to $5 \times 10^{-4}\,h^{-1}$, since the rilpivirine formulation included in LATTE-2 was different from previous investigation and [19] with a slower release rate [1]. A schematic of the LATTE-2 dosing regimen implemented in this study is shown in Fig 2.

2.4 Dose prediction

After the validation of the physicochemical parameters, the anatomy and physiology were modified to describe children and adolescents using appropriate allometric equations obtained from the literature, as described in the Online Resource 1 [12, 23, 25-27, 39, 40]. Following IM injection, dose optimisation in healthy paediatric individuals was conducted such that at least 95 out of the 100 virtual individuals had a mean trough concentration (C_{trough}) over the target trough concentrations for the required duration. Based on the LATTE-2 study, a target C_{trough} of 1.35 µg/ml was used as the minimum target trough concentration for cabotegravir dose predictions following 10 mg oral dose, and 70 ng/ml was used as the average concentration (C_{av}) for rilpivirine following a 25 mg dose [19]. An oral dosing regimen for 4 weeks (steady state) followed by a loading dose and eleven maintenance doses for a 4-weekly IM administration of rilpivirine and cabotegravir were simulated, for a total period of 52 weeks.

2.5 Sensitivity analysis

A differential sensitivity analysis was performed to identify the key parameters that impact the pharmacokinetic profiles of LA formulations [41]. Analysis was performed for the loading dose and the first maintenance dose of cabotegravir and rilpivirine LAI IM formulation in adults. Sensitivity was analysed using the provided inbuilt feature of Simbiology at user-defined values without normalisation in the computation. Six parameters – blood-to-plasma ratio, cardiac output, plasma clearance, liver weight, fraction unbound and release rate were analysed against drug plasma concentrations. Each parameter was varied by 20% from its mean value and 100 simulations were conducted while keeping the rest of the parameters constant. The sensitivity coefficient (ϕ_i) indicates the change of plasma concentration values (Y) with respect to a unit change in a parameter (X) as shown in equation 1 [41].

$$\emptyset_i = \frac{\%\Delta Y}{\%\Delta X} \quad (1)$$

3. Results

The structure and equation of the current PBPK model are based on a previous publication and modified to represent antiretroviral distribution in paediatric and adolescent individuals [21]. The anatomy and physiology of children and adolescents was also validated against literature and the results are presented in Online Resources 1. PBPK models were initially qualified by validation against available clinical data for both cabotegravir and rilpivirine in adults to ensure that the selected drug properties were appropriate. The mean simulated pharmacokinetic parameters for maximum concentration (C_{max}), C_{trough} and area under the concentration-time curve (AUC) were compared against available clinical data for the LA formulations for both drugs used in adults (cabotegravir – second IM dose of 800 mg and rilpivirine – 900 mg after the initial dose of 1200 mg) (shown in Table 2 and Fig. 1). A stringent qualification of accuracy was applied whereby PBPK models were considered validated only if the mean value was within 0.5-fold from the clinical value, rather than the conventional 2-fold agreement limits [42].

The formulation characteristics were maintained equal to the adult formulation for the simulations in children and adolescents assuming a similar release rate of the drugs from the formulations, and the use of the same formulations in adult, children and adolescents. IM doses were optimised to have a pharmacokinetic profile with concentration exceeding the 10 mg PO C_{trough} for cabotegravir over the duration of treatment and an average concentration over the C_{trough} of 25 mg PO rilpivirine for the first 12 IM doses (Fig. 3). For rilpivirine, it was also ensured that the concentrations were always above the 90% protein binding adjusted inhibitory concentration ($PAIC_{90}$) value of 12.1 ng/ml [18] subsequent to the loading dose. Summary of predicted doses for both cabotegravir and rilpivirine for different weight categories are shown in Table 3.

3.1 Cabotegravir

The validation for 800 mg IM cabotegravir resulted in mean predicted AUC, C_{max} and C_{trough} values that were +15.6 %, +6.1 % and +9.1 % compared to clinical values, respectively [1]. A target trough concentration of 1.35 µg/ml (10 mg PO C_{trough}) was chosen from the literature [1]. The doses for different weight groups were informed such that at least 95 out of the 100 virtual individuals had a C_{trough} value over the target trough concentration for a duration of 48 weeks (Fig 4). The daily oral dose administered for a period of 4 weeks was 10 mg for weights ranging between 14-50 kg and 20 mg for weights between 50-70 kg. For IM cabotegravir, the loading dose ranged between 200-600 mg and maintenance doses between 100-250 mg for the simulated plasma C_{trough} to stay over the 10 mg PO C_{trough} as described in Table 3.

3.2 Rilpivirine

The simulated mean AUC, C_{max} and C_{trough} values were +13.2 %, -6.5 % and -8.8 %, compared to the clinical data [1]. After the validation of rilpivirine PBPK model, the first order kinetic release rate was identified to be $9 \times 10^{-4}\ h^{-1}$ [1]. The validation was then performed to find the optimal release rate for rilpivirine pharmacokinetics from the LATTE-2 study. Due to reformulation of the rilpivirine, the optimal release rate was observed to be $5 \times 10^{-4}\ h^{-1}$. The optimal doses were informed for different weight categories such that the average drug C_{trough} plasma concentrations of 48 weeks remained over 70 ng/ml (25 mg PO C_{trough}) [19]. A fixed daily oral dose of 25 mg was administered for 4 weeks prior to IM doses. The loading dose ranged from 250 – 550 mg and the maintenance doses from 200 – 500 mg across weight groups from 15-70 kg individuals. The optimal doses ensured plasma concentrations over the $PAIC_{90}$ value and average IM concentrations over 25 mg PO C_{trough} for at least 95 out of 100 individuals (Fig 5).

3.3 Sensitivity Analysis

Fig. 6 shows the mean differential sensitivity analysis plot of 100 runs for six chosen parameters with respect to time. The analysis was performed for two successive (loading and maintenance) monthly IM doses of cabotegravir and rilpivirine in adults.

For cabotegravir, the analysis indicated that the plasma concentration is sensitive to only two of the six factors and higher influence was observed in the first days following administration. Cardiac output and systemic clearance of drug had higher sensitivity towards the variation in plasma concentrations. Protein binding, release rate, liver weight and blood-to-plasma ratio were negligibly sensitive. This indicates that physiological factors and the UGT content in the liver had a higher potential to influence the simulated pharmacokinetics. Sensitivity against cardiac output was negative for most of the duration indicating an increased effect against plasma concentration even when the value changes by ± 20% from the mean. Sensitivity against systemic clearance had a similar trend to cardiac output but with lower intensity. During the initial days after the administration of the maintenance dose, both these factors showed a positive relationship against plasma concentration indicating a lower effect.

For rilpivirine, the change in plasma concentration was not sensitive when cardiac output, liver weight and release rate varied ± 20 % from the mean. Blood-to-plasma ratio had a higher positive effect immediately after dosing implying a lower influence on plasma concentration. Blood-to-plasma ratio and systemic clearance showed a positive relationship over the entire dosing period indicating a decreased effect against plasma concen-

tration. Protein binding fluctuated between positive and negative, however the variation is minimal signifying minimal or no effect on plasma concentration.

4. Discussion

Optimal treatment adherence is essential for effective inhibition of viral replication and to mitigate development of resistance to ARVs. Although oral formulations have been demonstrated to result in therapeutic concentrations, sub-optimal adherence in patients who are receiving oral daily dosing for treatment and prevention have been described [2, 43-46]. Alternative administration strategies could support higher adherence reducing the frequency of administration and addressing pill fatigue. More specifically, formulations allowing a monthly or quarterly administration could address the adherence issue, thus decreasing the risk of drug resistance. ARVs with high potency and favourable pharmacokinetics are essential for the development of the LAI strategy. The recent development of novel formulations of cabotegravir and rilpivirine constitute a remarkable step towards the definition of LAI strategies, providing innovative pharmacological tools for adults [1]. Dose optimisation in special populations of patients such as children and adolescents is complex due to their unique physiological and anatomical characteristics compared to adults. Traditionally, clinical trials have not been frequently conducted in these patient populations due to ethical and logistical considerations [47]. However recent regulations promote clinical studies in paediatric patients to evaluate safety and efficacy prior to therapy [48, 49]. The present study focuses on the identification of dosing strategies of cabotegravir and rilpivirine in children and adolescents using computational PK modelling for HIV treatment.

Various PBPK models have been developed for adults and recently this modelling technique has also been used for a variety of special populations including children and adolescents [50, 51]. Drug distribution can be simulated in special populations of patients through the integration of age-related anatomical and physiological changes into the mathematical PBPK framework. PBPK modelling has been recently used for the prediction of midazolam and theophylline in neonates, infants and children [12]. In two other studies, the relationship between adult and paediatric clearance rates was established using cytochrome P450 ontogeny for six compounds and then simulations were performed for five different drugs at different age groups [52, 53]. An oseltamivir PBPK model was used to predict pharmacokinetics in neonates and infants with influenza [54] and a disease-specific model was also recently developed in children with and without liver cirrhosis [55].

Both cabotegravir and rilpivirine are characterised by long-half lives and physicochemical properties that are compatible with nanoformulations for LAIs, represent attractive options for continuous therapy [1, 56]. Using physiochemical properties and *in vitro* data, the pharmacokinetics of cabotegravir and rilpivirine in adults was validated against available clinical data. The model validation was conducted at the second dose of the LAI

ARVs to have a mathematical representation of the pharmacokinetics at steady-state. Low accuracy and precision was observed in the ÉCLAIR study where the simulated C_{trough} value of cabotegravir was 1.35 µg/ml compared to the observed value which was less than 0.66 µg/ml (4*$PAIC_{90}$)[57]. Hence, stringent guidelines were applied for the validation process where ± 50 % deviation from the mean clinical values was considered acceptable instead of the conventional 2-fold deviation [42]. The pharmacokinetic parameters – AUC, C_{max} and C_{trough} simulated through the PBPK approach were in agreement with the clinical data and therefore our PBPK model was considered robust for predicting the LAI IM doses in children and adolescents. In the simulation of LAI pharmacokinetics in children, the release rates of the LAI formulations were maintained equal to the validation in adults, to facilitate bridging to paediatric simulation. Although the physiology of the muscular tissues is different between adults and children, this could potentially support the use of the existing formulations in paediatric clinical studies with no further reformulation [58]. However additional studies are required since there is a possibility that smaller doses with less injection volume could decrease total surface area and strain in the muscle, thereby altering the pharmacokinetic profile. The doses were optimised such that cabotegravir and rilpivirine concentrations were over the target trough concentrations (described in methods section) for the duration of the dose. Although $PAIC_{90}$ values indicate a trough concentration to suppress the virus *in vitro*, this does not translate in effective therapeutic activity *in vivo* [59]. Therefore, the dose optimisation was conducted considering LATTE-2 study target trough concentrations.

The required dose was proportional to the weight of the individual which indicates increase in volume of distribution and systemic clearance in adolescents. As the weight of the individual increased from 15 to 70 kg, the required dose of cabotegravir tripled in an individual weighing 70 kg compared to a 15 kg individual whereas the dose needed was just over double in the case of rilpivirine. Fluctuation in maximum and trough plasma concentration of cabotegravir is >2 µg/ml compared to rilpivirine (<100 ng/ml). Also cabotegravir is more sensitive to variations in clearance and cardiac output compared to rilpivirine (as shown in Fig. 6) and due to these physiological variations across weight groups, higher dose is required in case of cabotegravir for adolescents compared to children. This indicates that doses cannot be linearly extrapolated based on weight and a deeper understanding of important mechanistic processes influencing the pharmacokinetics in children and adolescents is required. The loading doses are higher compared to the maintenance doses as the extra dose is essential to maintain drug plasma concentrations over the $C_{trough}/PAIC_{90}$ values. Since the maintenance dose for cabotegravir is low compared to rilpivirine, they could be more suitable for a less frequent (bimonthly or quarterly) administration.

LAI formulations may improve the problems faced with low adherence of therapies in children and adolescents. The identification of optimal doses in healthy paediatric individuals should be given priority as most of the doses for prescribed drugs are simply scaled from adult doses with varying success. However pain involved during the administration of IM injections has the potential to refrain children from preferring this route and opting for oral dosing regimens. Chloramphenicol dose scaling from adults in neonates and infants reached toxic levels which led to higher mortality rate, an example where the developmental pharmacology of paediatric patients was ignored [60]. Mortality rate was high in neonates affected with kernicterus who were administered penicillin/sulfisoxazole than with oxytetracycline in an another case [61]. In both these cases, an immature glucuronidation system led to the accumulation of drug, resulting in high plasma concentrations and conclusively demonstrating that the physiological processes of the child cannot always be accounted for by scaling adult doses [61, 62].

Although the simulated doses for children and adolescents could represent a valuable guideline for drug safety and efficacy clinical studies, the applied modelling strategies have some limitations. Numerous barriers can complicate the implementation of dosing recommendations for special populations. Since anatomical and physiological changes in children follow non-linear trend, pharmacokinetic, pharmacodynamic investigations need to be conducted to evaluate the safety, efficacy and tolerability profiles in children and the current modelling approach can support a rational identification of suitable dosing strategies [63]. Especially in infants and neonates younger than three years, ontogeny of CYP450 expression in the liver and wide variation in organ weights and volumes could lead to low accuracy in model prediction and hence this study focuses on children older than three years. Some anatomical and physiological features and the associated complex biological processes have not been simulated due to a paucity of relevant data [35]. Absence of information on drug transporters at the injection site could alter the absorption, distribution and metabolic processes which could not be captured in the current PBPK model. Evidence suggests that cabotegravir undergoes enterohepatic recirculation, however quantitative evaluation of this physiological process is absent and hence could not be incorporated in the PBPK model [64]. Recent investigation with paliperidone LAI micro suspension revealed formation of a granuloma due to macrophage accumulation surrounding the site of injection. This phenomenon further controlled drug release from the depot and evidence also showed drug uptake and release from macrophages [65]. The extent of the occurrence of this phenomenon and the size of the depot could alter the release rates and thereby drug pharmacokinetics which was not accounted for in this study. Physiological and metabolic variation of muscle composition in children compared to adults was not accounted during the dose optimisation process

[58]. Low clinical C_{max} compared to the simulated pharmacokinetic curve (Fig. 1) could be due to the fraction of drug distributed through the lymphatic circulation. Additionally, the potential adverse effects considering the differences in the anatomy and physiology of children compared to adults, prolonged exposure and inability to discontinue therapy once administered are important factors to be assessed before drug administration [3].

LAI therapy has attracted a great deal of attention in various therapeutic areas, including chronic HIV infection. For example, the National Institutes of Health (NIH) recently provided support to set up a worldwide team involving researchers from academia and the pharmaceutical industry to facilitate development of LAI formulations for HIV. This Long-Acting/Extended Release Antiretroviral Resource Program (LEAP; www.longactinghiv.org) includes a PBPK modelling service to facilitate the design of long-acting formulations for HIV and related infectious diseases. This kind of support may improve the efficiency of selection of formulations, doses, and dose intervals for paediatric and other special populations.

5. Conclusion

PBPK models were successfully validated for both cabotegravir and rilpivirine LAI formulations against available clinical data in adults. A novel PBPK model for the prediction of PK in children and adolescent individuals was developed to simulate dose selection in this vulnerable group. Dosing strategies for cabotegravir and rilpivirine were estimated in different weight groups of children and adolescents considering two efficacy target trough concentrations. From this modelling study, the predicted paediatric dosing of caboteravir and rilpivirine differ for each weight category and scaling adult dose could have led to plasma concentration either below $PAIC_{90}$/MEC value or above safe level. Different dosing fractions compared to adult dosages for cabotegravir and rilpivirine indicate that drug specific physiocochemical parameters and ADME characteristics play a key role in controlling pharmacokinetics. PBPK predictions from this study could potentially inform reference doses required to conduct paediatric clinical trials for various weight categories.

Compliance with ethical standards:

Source of Funding:

This work was supported by the National Institutes of Health (R24 AI 118397).

Conducting of research:

Rajith KR Rajoli has done the PBPK modelling. Rajith KR Rajoli and Marco Siccardi have written the manuscript. David J Back, Steve Rannard, Caren Freel Meyers, Charles Flexner and Andrew Owen have reviewed the manuscript.

Conflict of Interest:

David J Back receives consulting or advisor fees from Abbvie, Boehringer Ingelheim, Gilead, Janssen, Merck and ViiV. He also received research funding from Abbvie, Boehringer Ingelheim, BMS, Gilead, Janssen, Merck and ViiV. Steve Rannard received funding from ViiV and AstraZeneca and have many HIV nanomedicine patents. Charles Flexner received consulting or advisor fees from Abbvie, Boehringer Ingelheim, Bristol Myers-Squibb, Gilead and GlaxoSmithKline, Merck and ViiV. Andrew Owen has received research funding from Merck, ViiV Healthcare, Janssen, Pfizer and AstraZeneca, consultancy from Merck and Norgine, and is a co-inventor of patents relating to HIV nanomedicines. Marco Siccardi has received research funding from ViiV and Janssen. Rajith KR Rajoli and Caren Freel Meyers have no conflicts of interest to declare.

6. Tables

Table 1 Physicochemical properties, *in vitro* and population pharmacokinetic data of ARVs

	Cabotegravir	**Rilpivirine**
Molecular weight	427	366
log $P_{o:w}$	1.04 [66]	4.32 [67]
Protein binding	99.30% [56]	99.70% [67]
pK_a	10.04 [66]	3.26 [67]
R	0.441 [68]	0.67 [67]
Polar surface area	99.2	-
Hydrogen bond donors	2	-
Caco-2 permeability (cm/s)	-	12×10^{-6} [67]
CYP3A4 CL_{int}	-	2.04 [67]
UGT1A1 CL_{int}	4.5 [37]	-
UGT1A9 CL_{int}	2.2 [37]	-
Release rate (h^{-1})	4.5×10^{-4} [36]	9×10^{-4} [1]

log $P_{o:w}$ – Partition coefficient between octanol and water; pKa – logarithmic value of the dissociation constant; R – blood-to-plasma drug ratio; CL_{int} – intrinsic clearance; CYP – cytochrome P450 (µl/min/pmol); UGT - uridine diphosphate glucuronosyltransferase (µl/min/mg)

Table 2 Validation of cabotegravir and rilpivirine after the second IM dose in adults: Clinical [1] vs. simulated pharmacokinetic data

Drug	Dose (mg)	AUC		C_{max}		C_{trough}	
		Clinical	**Predicted**	**Clinical**	**Predicted**	**Clinical**	**Predicted**
Cabotegravir	800 mg quarterly	4467 (52)	5166 (23)	3.3 (59)	3.5 (21)	1.1 (140)	1.2 (24)
Rilpivirine	900 mg monthly	74,420 (35)	84,270 (44)	168 (37)	157 (42)	79.1 (44)	72.1 (45)

Values are represented as Geometric mean (% CV – coefficient of variation expressed as a percentage), AUC – area under the concentration-time curve, C_{max} – maximum plasma concentration, C_{trough} – trough plasma concentration. For Cabotegravir C_{max} and C_{trough} are µg/ml and AUC is µg × h/ml at day 84. For rilpivirine C_{max} and C_{trough} are ng/ml and AUC is ng × h/ml at day 28

Table 3 Prediction of the dose (in mg) for cabotegravir and rilpivirine for different weight categories of children and adolescents with initial 4 weeks of oral dose followed by IM loading dose and 11 maintenance doses lasting 4-weeks each

Weight (kg)	**Rilpivirine**			**Cabotegravir**		
	Oral	**Loading dose**	**Maintenance dose**	**Oral**	**Loading dose**	**Maintenance dose**
14 - 19.9	25	250	150	10	200	100
20 - 24.9		250	200		250	100
25 - 29.9		250	200		250	100
30 - 34.9		300	250		350	150
35 - 39.9		350	300		350	150
40 - 44.9		400	300		400	150
45 - 49.9		450	350		450	150
50 - 54.9		450	400	20	450	200
55 - 59.9		500	400		500	200
60 - 64.9		500	450		550	200
65 - 69.9		550	500		600	250
Target concentration in ng/ml (achieved by a PO dose in mg) [Reference]	70 (25 mg PO C_{trough}) [19]			1370 (10 mg PO C_{trough}) [19]		

PO – oral route, C_{trough} – trough concentration

References

1. Spreen W, Williams P, Margolis D, Ford SL, Crauwels H, Lou Y, et al. Pharmacokinetics, Safety, and Tolerability With Repeat Doses of GSK1265744 and Rilpivirine (TMC278) Long-Acting Nanosuspensions in Healthy Adults. Jaids-Journal of Acquired Immune Deficiency Syndromes. 2014 Dec 5;67(5):487-92.
2. Chesney MA. Factors Affecting Adherence to Antiretroviral Therapy. Clinical Infectious Diseases. 2000 June 1, 2000;30(Supplement 2):S171-S6.
3. Spreen WR, Margolis DA, Pottage JCJ. Long-acting injectable antiretrovirals for HIV treatment and prevention. Curr Opin HIV AIDS. 2013;8(6):565-71.
4. Haberer J, Mellins C. Pediatric Adherence to HIV Antiretroviral Therapy. Current HIV/AIDS reports. 2009;6(4):194-200.
5. Owen S. Muir AA-J, Padam Bhatia, MD, Sandeep Kapoor, John Kane, Christoph U. Correll. Attitudes of Children and Adolescents and Their Caregivers Towards Long-Acting Injectable Antipsychotics in a Cohort of Youth Initiating Oral Antipsychotic Treatment. 60th Annual Meeting - American Academy of Child Adolescent Psychiatry. Orlando, FL; 2013.
6. Pope S, Zaraa SG. Efficacy of Long-Acting Injectable Antipsychotics in Adolescents. Journal of Child and Adolescent Psychopharmacology. 2016 2016/05/01;26(4):391-4.
7. Fàbrega M, Sugranyes G, Baeza I. Two cases of long-acting paliperidone in adolescence. Therapeutic Advances in Psychopharmacology. 2015;5(5):304-6.
8. van ′t Klooster G, Hoeben E, Borghys H, Looszova A, Bouche M-P, van Velsen F, et al. Pharmacokinetics and Disposition of Rilpivirine (TMC278) Nanosuspension as a Long-Acting Injectable Antiretroviral Formulation. Antimicrob Agents Chemother 2010 May 1, 2010;54(5):2042-50.
9. Healthcare V. A Phase IIb Study to Evaluate a Long-Acting Intramuscular Regimen for Maintenance of Virologic Suppression (Following Induction With an Oral Regimen of GSK1265744 and Abacavir/Lamivudine) in Human Immunodeficiency Virus Type 1 (HIV-1) Infected, Antiretroviral Therapy-Naive Adult Subjects. 2014 04/02/2016 [cited 2016 15/03/2016]; Available from: https://clinicaltrials.gov/ct2/show/NCT02120352
10. Margolis DA, Brinson CC, Smith GHR, de Vente J, Hagins DP, Eron JJ, et al. Cabotegravir plus rilpivirine, once a day, after induction with cabotegravir plus nucleoside reverse transcriptase inhibitors in antiretroviral-naive adults with HIV-1 infection (LATTE): a randomised, phase 2b, dose-ranging trial. The Lancet Infectious Diseases. 2015 10//;15(10):1145-55.
11. Leong R, Vieira MLT, Zhao P, Mulugeta Y, Lee CS, Huang SM, et al. Regulatory Experience With Physiologically Based Pharmacokinetic Modeling for Pediatric Drug Trials. Clinical Pharmacology & Therapeutics. 2012;91(5):926-31.
12. Bjorkman S. Prediction of drug disposition in infants and children by means of physiologically based pharmacokinetic (PBPK) modelling: theophylline and midazolam as model drugs. Br J Clin Pharmacol. 2005 Jun;59(6):691-704.
13. Neely M, Margol A, Fu XW, van Guilder M, Bayard D, Schumitzky A, et al. Achieving Target Voriconazole Concentrations More Accurately in Children and Adolescents. Antimicrobial Agents and Chemotherapy. 2015 Jun;59(6):3090-7.
14. Philippe M, Neely M, Bertrand Y, Bleyzac N, Goutelle S. A Nonparametric Method to Optimize Initial Drug Dosing and Attainment of a Target Exposure Interval: Concepts and Application to Busulfan in Pediatrics. Clinical Pharmacokinetics. 2016 2016:1-13.
15. Bouazza N, Cressey TR, Foissac F, Bienczak A, Denti P, McIlleron H, et al. Optimization of the strength of the efavirenz/lamivudine/abacavir fixed-dose combination for paediatric patients. Journal of Antimicrobial Chemotherapy. 2016 October 24, 2016.
16. Bouazza N, Foissac F, Fauchet F, Burger D, Kiechel JR, Treluyer JM, et al. Lopinavir/ritonavir plus lamivudine and abacavir or zidovudine dose ratios for paediatric fixed-dose combinations. Antiviral Therapy. 2015;20(2):225-33.
17. Siccardi M, Rajoli RKR, Curley P, Olagunju A, Moss D, Owen A. Physiologically based pharmacokinetic models for the optimization of antiretroviral therapy: recent progress and future perspective. Future Virol 2013 2013/09/01;8(9):871-90.
18. Jackson AGA, Else LJ, Mesquita PMM, Egan D, Back DJ, Karolia Z, et al. A Compartmental Pharmacokinetic Evaluation of Long-Acting Rilpivirine in HIV-Negative Volunteers for Pre-Exposure Prophylaxis. Clinical Pharmacology & Therapeutics. 2014;96(3):314-23.
19. David A. Margolis DP, Hans-Jurgen Stellbrink, Thomas Lutz, Jonathan B. Angel, Gary Richmond, Bonaventura Clotet, Felix Gutierrez, Louis Sloan, Sandy K. Griffith, Marty St Clair, David Dorey, Susan Ford, Joseph Mrus, Herta Crauwels, Kimberly Y. Smith, Peter E. Williams, William R. Spreen. Cabotegravir +

Rilpivirine as Long-Acting Maintenance Therapy: LATTE-2 Week 48 Results International AIDS Conference; 2016; Durban, South Africa; 2016.
20. Nestorov I. Whole Body Pharmacokinetic Models. Clinical Pharmacokinetics. 2003 2003//;42(10):883-908.
21. Rajoli RKR, Back DJ, Rannard S, Freel Meyers CL, Flexner C, Owen A, et al. Physiologically Based Pharmacokinetic Modelling to Inform Development of Intramuscular Long-Acting Nanoformulations for HIV. Clinical Pharmacokinetics. 2014;54(6):639-50.
22. WHO. Antiretroviral therapy for hiv infection in infants and children: Towards universal access; 2010.
23. Bosgra S, Eijkeren Jv, Bos P, Zeilmaker M, Slob W. An improved model to predict physiologically based model parameters and their inter-individual variability from anthropometry. Crit Rev Toxicol. 2012;42(9):751-67.
24. Chamberlain JM, Capparelli EV, Brown KM, Vance CW, Lillis K, Mahajan P, et al. Pharmacokinetics of Intravenous Lorazepam in Pediatric Patients with and without Status Epilepticus. The Journal of Pediatrics. 2012 4//;160(4):667-72.e2.
25. Centers for Disease Control and Prevention. CDC growth charts: United States; 2000 May 30, 2000.
26. Price PS, Conolly RB, Chaisson CF, Gross EA, Young JS, Mathis ET, et al. Modeling Interindividual Variation in Physiological Factors Used in PBPK Models of Humans. Critical Reviews in Toxicology. 2003 2003/01/01;33(5):469-503.
27. Haddad S, Restieri C, Krishnan K. Characterization of age-related changes in body weight and organ weights from birth to adolescence in humans. Journal of Toxicology and Environmental Health-Part A. 2001 Nov 23;64(6):453-64.
28. Shankle WR, Landing BH, Gregg J. Normal organ weights of infants and children: graphs of values by age, with confidence intervals. Pediatric pathology / affiliated with the International Paediatric Pathology Association. 1983 1983;1(4).
29. McQueen CA, Bond J, Ramos K, Lamb J, Guengerich FP, Lawrence D, et al. Comprehensive Toxicology, Volumes 1-14 (2nd Edition). Elsevier.
30. Ginsberg G, Hattis D, Russ A, Sonawane B. Physiologically Based Pharmacokinetic (PBPK) Modeling of Caffeine and Theophylline in Neonates and Adults: Implications for Assessing Children's Risks from Environmental Agents. Journal of Toxicology and Environmental Health, Part A. 2004 2004/02/01;67(4):297-329.
31. Williams LR. Reference values for total blood volume and cardiac output in humans; 1994.
32. Maharaj AR, Barrett JS, Edginton AN. A Workflow Example of PBPK Modeling to Support Pediatric Research and Development: Case Study with Lorazepam. AAPS J. 2013;15(2):455-64.
33. DrugBank. Lorazepam. 2013 [cited 2016 13/5/2016]; Available from: http://www.drugbank.ca/drugs/DB00186
34. Dajani AS, Thirumoorthi MC, Bawdon RE, Buckley JA, Pfeffer M, Van Harken DR, et al. Pharmacokinetics of intramuscular ceforanide in infants, children, and adolescents. Antimicrobial Agents and Chemotherapy. 1982 February 1, 1982;21(2):282-7.
35. Tegenge M, Mitkus R. A physiologically-based pharmacokinetic (PBPK) model of squalene-containing adjuvant in human vaccines. J Pharmacokinet Pharmacodyn. 2013 2013/10/01;40(5):545-56.
36. Ford SL, Chen J, Lovern M, Spreen W, Kim J. Population PK Approach to Predict Cabotegravir (CAB, GSK1265744) Long-Acting Injectable Doses for Phase 2b. ICAAC; 2014; Washington, DC; 2014.
37. Reese M FS, Bowers G, Humphreys J, Webster L, Gould E, Polli J, Generaux G, Johnson M, Clark P, Watson C, Lou Y, Piscitelli S. In Vitro Drug Interaction Profile of the HIV Integrase Inhibitor, GSK1265744, and Demonstrated Lack of Clinical Interaction with Midazolam. 15th International Workshop on Clinical Pharmacology of HI V and Hepatitis Therapy; 2014; Washington, DC; 2014.
38. Iwatsubo T, Hirota N, Ooie T, Suzuki H, Shimada N, Chiba K, et al. Prediction of in vivo drug metabolism in the human liver from in vitro metabolism data. Pharmacology & Therapeutics. 1997 //;73(2):147-71.
39. Shankle WR, Landing BH, Gregg J. Normal organ weights of infants and children: graphs of values by age, with confidence intervals. Pediatric pathology / affiliated with the International Paediatric Pathology Association. 1983 1983;1(4):399-408.
40. Comprehensive Toxicology, Vol 12: Developmental Toxicology, 2nd Edition; 2010.
41. Hamby DM. A review of techniques for parameter sensitivity analysis of environmental-models. Environmental Monitoring and Assessment. 1994 Sep;32(2):135-54.
42. Abduljalil K, Cain T, Humphries H, Rostami-Hodjegan A. Deciding on Success Criteria for Predictability of Pharmacokinetic Parameters from In Vitro Studies: An Analysis Based on In Vivo Observations. Drug Metab Dispos 2014 July 2, 2014.
43. Wakibi SN, Ng'ang'a ZW, Mbugua GG. Factors associated with non-adherence to highly active antiretroviral therapy in Nairobi, Kenya. AIDS Research and Therapy. 2011;8(1):1-8.

44. Hansana V, Sanchaisuriya P, Durham J, Sychareun V, Chaleunvong K, Boonyaleepun S, et al. Adherence to Antiretroviral Therapy (ART) among People Living With HIV (PLHIV): a cross-sectional survey to measure in Lao PDR. BMC Public Health. 2013;13(1):1-11.
45. Simoni JM, Montgomery A, Martin E, New M, Demas PA, Rana S. Adherence to antiretroviral therapy for pediatric HIV infection: A qualitative systematic review with recommendations for research and clinical management. Pediatrics. 2007 Jun;119(6):E1371-E83.
46. Buchanan AL, Montepiedra G, Sirois PA, Kammerer B, Garvie PA, Storm DS, et al. Barriers to Medication Adherence in HIV-Infected Children and Youth Based on Self- and Caregiver Report. Pediatrics. 2012 01/12/accepted;129(5):e1244-e51.
47. Barrett JS, Della Casa Alberighi O, Läer S, Meibohm B. Physiologically Based Pharmacokinetic (PBPK) Modeling in Children. Clinical Pharmacology & Therapeutics. 2012;92(1):40-9.
48. EMEA. Regulation (EC) no 1901 / 2006 of the European Parliament and of the Council on medicinal products for paediatric use and amending Regulation (EEC) No 1768 / 92, Directive 2001 / 20/EC, Directive 2001 / 83/EC and Regulation (EC) No 726 / 2004.; 2006.
49. Congress U. Pediatric Research Equity Act of 2003; 2003.
50. Ginsberg G, Hattis D, Russ A, Sonawane B. Physiologically based pharmacokinetic (PBPK) modeling of caffeine and theophylline in neonates and adults: Implications for assessing children's risks from environmental agents. Journal of Toxicology and Environmental Health-Part a-Current Issues. 2004 Feb 27;67(4):297-329.
51. Maharaj AR, Barrett JS, Edginton AN. A Workflow Example of PBPK Modeling to Support Pediatric Research and Development: Case Study with Lorazepam. The AAPS Journal. 2013;15(2):455-64.
52. Edginton AN, Schmitt W, Willmann S. Development and Evaluation of a Generic Physiologically Based Pharmacokinetic Model for Children. Clinical Pharmacokinetics. 2012;45(10):1013-34.
53. Edginton AN, Schmitt W, Voith B, Willmann S. A Mechanistic Approach for the Scaling of Clearance in Children. Clinical Pharmacokinetics. 2012;45(7):683-704.
54. Parrott N, Davies B, Hoffmann G, Koerner A, Lave T, Prinssen E, et al. Development of a Physiologically Based Model for Oseltamivir and Simulation of Pharmacokinetics in Neonates and Infants. Clinical Pharmacokinetics. 2011;50(9):613-23.
55. Edginton AN, Willmann S. Physiology-Based Simulations of a Pathological Condition. Clinical Pharmacokinetics. 2008;47(11):743-52.
56. Trezza C, Ford SL, Spreen W, Pan R, Piscitelli S. Formulation and pharmacology of long-acting cabotegravir. Current Opinion in Hiv and Aids. 2015 Jul;10(4):239-45.
57. Martin Markowitz IF, Robert Grant, Kenneth H. Mayer, David A. Margolis, Krischan J. Hudson, Britt S. Stancil, Susan L. Ford, Alex R. Rinehart, William Spreen. ÉCLAIR: Phase 2A Safety and PK Study of Cabotegravir LA in HIV-Uninfected Men. Conference on Retroviruses and Opportunistic Infections; 2016; Boston; 2016.
58. Dotan R, Mitchell C, Cohen R, Klentrou P, Gabriel D, Falk B. Child—Adult Differences in Muscle Activation — A Review. Pediatric exercise science. 2012;24(1):2-21.
59. Acosta EP, Limoli KL, Trinh L, Parkin NT, King JR, Weidler JM, et al. Novel Method To Assess Antiretroviral Target Trough Concentrations Using In Vitro Susceptibility Data. Antimicrob Agents Chemother. 2012 November 1, 2012;56(11):5938-45.
60. Weiss CF, Glazko AJ, Weston JK. Chloramphenicol in the Newborn Infant. New England Journal of Medicine. 1960;262(16):787-94.
61. Silverman WA, Andersen DH, Blanc WA, Crozier DN. A Difference In Mortality Rate and Incidence of Kernicterus among Premature Infants Allotted to Two Prophylactic Antibacterial Regimens. Pediatrics. 1956;18(4):614.
62. Mahmood I. Dosing in Children: A Critical Review of the Pharmacokinetic Allometric Scaling and Modelling Approaches in Paediatric Drug Development and Clinical Settings. Clinical Pharmacokinetics. 2014;53(4):327-46.
63. Services USDoHaH. General Clinical Pharmacology Considerations for Pediatric Studies for Drugs and Biological Products 2014.
64. Bowers GD, Culp A, Reese MJ, Tabolt G, Moss L, Piscitelli S, et al. Disposition and metabolism of cabotegravir: a comparison of biotransformation and excretion between different species and routes of administration in humans. Xenobiotica. 2016 2016/02/01;46(2):147-62.
65. Darville N, van Heerden M, Vynckier A, De Meulder M, Sterkens P, Annaert P, et al. Intramuscular Administration of Paliperidone Palmitate Extended-Release Injectable Microsuspension Induces a Subclinical Inflammatory Reaction Modulating the Pharmacokinetics in Rats. Journal of Pharmaceutical Sciences. 2014;103(7):2072-87.
66. Chemaxon. Chemicalize.org, Properties viewer. 2016 [cited 2016 18/03/2016]; Available from: http://www.chemicalize.org/

67. Application number: 202022Orig1s000. Clinical Pharmacology and Biopharmaceutics Review(s). Center for Drug Evaluation and Research; 2011.
68. A Culp GB, E Gould, S Ford, Y Lou, R Pan, D Margolis, S Piscitelli. Metabolism, Excretion, and Mass Balance of the HIV Integrase Inhibitor, Cabotegravir (GSK1265744) in Humans. ICAAC 2014 54th Interscience Conference on Antimicrobial Agents and Chemotherapy; 2014; Washington, DC; 2014.

Figure Legends

Figure 1 Validation of the PBPK model parameters against clinical data for the second IM administration in adults. a) Cabotegravir (800 mg followed by 800 mg quarterly) b) Rilpivirine (1200 mg followed by 900 mg monthly) [1]

Figure 2 Validation of adult PBPK model using LATTE-2 dosing regimen. Oral dosing regimen was followed for 4 weeks, followed by a single 4-weekly intramuscular dose and eleven 4-weekly intramuscular maintenance doses. CAB – cabotegravir, RPV – rilpivirine, QD – once daily, Q4W – 4-weekly dose

Figure 3 Validation of the release rate against clinical data from 48-week LATTE-2 study in adults. a) Cabotegravir b) Rilpivirine [19]. The target trough concentration is 1.35 µg/ml for cabotegravir and 12 ng/ml for rilpivirine

Figure 4 Plasma concentrations of cabotegravir loading and maintenance doses from week 4 to week 52 for different weight categories of children and adolescents. a) 14 - 19.9 kg, b) 25 - 29.9 kg, c) 35 - 39.9 kg, d) 45 - 49.9 kg, e) 55 - 59.9 kg and f) 65 - 69.9 kg. The mean plasma concentrations are over the target trough concentrations of 1.37 µg/ml. Concentration data were derived from optimized dosing strategies calculated for each weight band, as described in the Results section.

Figure 5 Plasma concentrations of rilpivirine loading and maintenance doses from week 4 to week 52 for different weight categories of children and adolescents. a) 14 - 19.9 kg, b) 25 - 29.9 kg, c) 35 - 39.9 kg, d) 45 - 49.9 kg, e) 55 - 59.9 kg and f) 65 - 69.9 kg. The mean plasma concentrations are over the target trough concentrations of 17 ng/ml. Concentration data were derived from optimized dosing strategies calculated for each weight band, as described in the Results section.

Figure 6 Differential sensitivity analysis of plasma concentration against key parameters (blood-plasma ratio, cardiac output, fraction unbound, liver weight, release rate and systemic clearance) in adults for the 4-weekly intramuscular loading dose and the first maintenance dose. a) Cabotegravir, b) Rilpivirine

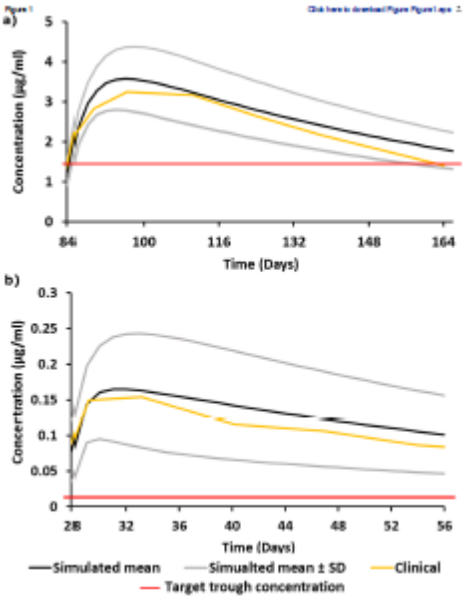
a)
Concentration (µg/ml)
0
1
2
3
4
5
84
100
116
132
148
164
Time (Days)
b)
Concentration (µg/ml)
0
0.05
0.1
0.15
0.2
0.25
0.3
28
32
36
40
44
48
52
56
Time (Days)
Simulated mean
Simualted mean ± SD
Clinical
Target trough concentration

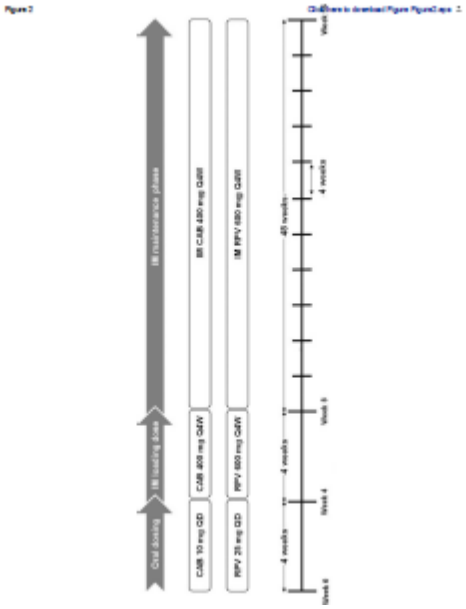
IM maintenance phase
IM CAB 400 mg Q4W
IM RPV 600 mg Q4W
IM loading dose
CAB 600 mg Q4W
RPV 600 mg Q4W
Oral dosing
CAB 30 mg QD
RPV 25 mg QD
48 weeks
4 weeks
4 weeks
4 weeks
Week 0
Week 4
Week 8
Week 12

Figure 3

Click here to download Figure Figure3.eps

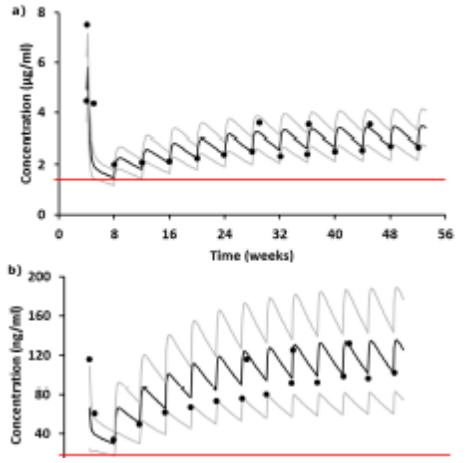

Figure 4

Click here to download Figure Figure4a.eps

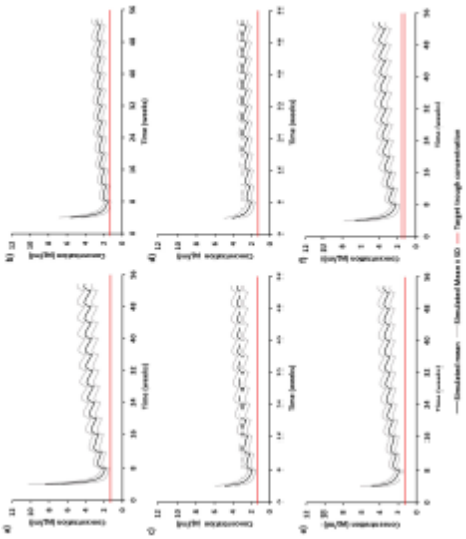

Figure 5

Click here to download Figure Figure5.eps

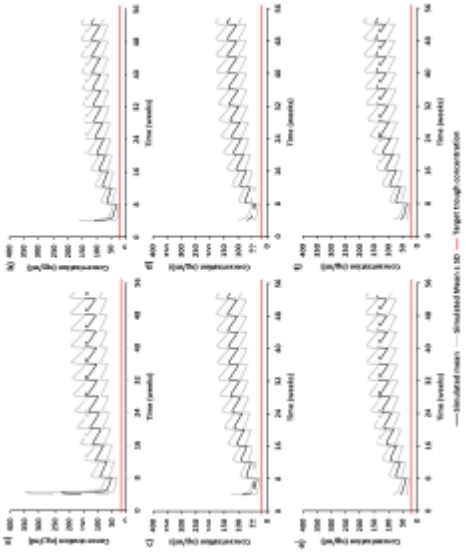

Figure 6

Click here to download Figure Figure6.eps

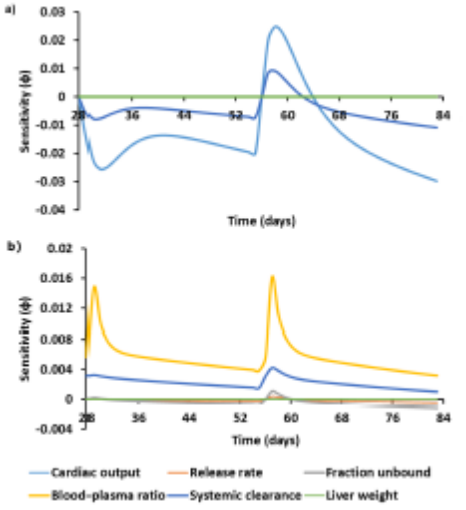

In silico dose prediction for long-acting rilpivirine and cabotegravir administration to children and adolescents

Journal: Clinical Pharmacokinetics

Rajith KR Rajoli[1], David J Back[1], Steve Rannard[2], Caren Freel Meyers[3], Charles Flexner[4], Andrew Owen[1], Marco Siccardi[1]

[1]Department of Molecular and Clinical Pharmacology, University of Liverpool, Liverpool, UK

[2]Department of Chemistry, University of Liverpool, Crown Street, Liverpool, UK

[3]Department of Pharmacology and Molecular Sciences, Johns Hopkins School of Medicine, Baltimore, MD, USA

[4]Johns Hopkins University School of Medicine and Bloomberg School of Public Health, Baltimore, MD, USA

Author for correspondence: Dr Marco Siccardi, Department of Molecular and Clinical Pharmacology, University of Liverpool, 70 Pembroke Place, Liverpool, L69 3GF, U.K.

Tel No +44 (0) 151 794 8211

Fax No + 44 (0) 151 794 5656

E-mail: siccardi@liverpool.ac.uk

Caption: PBPK model development and validation for paediatrics

1. Methods

Anatomy and physiology of children between the ages 2-18 years were validated. The simulated pharmacokinetics were validated against published clinical data for lorazepam, an anti-anxiety agent and ceforanide, an anti-bacterial agent as model drugs [1, 2]. The physicochemical and drug specific parameters values were identified using standardised terminology. For the reported drugs, only a single value for each parameter could be identified.

1.1 Anatomy

The weight and body mass index of the individuals were defined using CDC growth charts. The charts were digitalised using plot digitizer tool and polynomial trend line feature in Microsoft excel was used to obtain the relation between age and other parameters [3]. Using these defined parameters as reference, height and body surface area [4] were calculated using allometric equations from the literature (Table 1).

1.2 Tissue and organ weights

The tissue and organ weights were computed using allometric equations. All the organ weights were validated against published data for both male and female populations at different age groups [5]. Summary of the equations used and their references are shown in Table 2a, 2b.

1.3 Blood flow

The cardiac output for different age groups was obtained from literature sources. The blood flow rates of various organs and tissues were adjusted as the percentage of cardiac output such that they match the clinical values [6]. The sum of blood flow passing through the gut, pancreas, spleen and stomach was considered as the portal vein blood flow rate for PBPK models. The blood flows were adjusted due to the unavailability of data in the literature (Table 3).

1.4 Validation of anatomy and physiology

The paediatric characteristics, individual tissue and organ weights and blood flows were validated against available literature data [5, 6]. Simulations were performed for a population (100 individuals) by including standard deviation from the literature or ± 20% was assumed if not available, in each age group and the mean value was validated against literature data for both male and female groups.

1.5 Pharmacokinetic validation

To improve the confidence of the constructed models, it was validated against lorazepam, an anti-anxiety drug [1]. This drug was chosen due to the availability of physicochemical and pharmacokinetic data required for the construction and validation of the PBPK model. Dose of 0.05 mg/kg to a maximum of 2 mg was administered intravenously and the pharmacokinetics were simulated for 100 male individuals in each age group. The PBPK model was also validated against a single intramuscular 20 mg/kg dose of an anti-bacterial agent, ceforanide [2]. Maximum concentration (C_{max}), area under the curve (AUC) and volume of distribution (V_d) were compared against clinical data [1, 2].

1.6 ADME characteristics

The equations describing the ADME processes defining PK were derived from previously published PBPK models [7, 8]. The physicochemical and intrinsic clearance values of lorazepam were obtained from Maharaj et al. [9] and the extrapolation to systemic clearance and the distribution of drug to different organs and tissues was computed using previously published equations [7, 10].

Table 1 Equations describing the anatomical characteristic features for paediatrics

	Sex	2-7 years	7-18 years
BMI	**Male**	(-2E-06*(Age*12)^3+0.0009*(Age*12)^2-0.096*(Age*12)+18.41) ± (4E-09*(Age*12)^4-3E-06*(Age*12)^3+0.0006*(Age*12)^2-0.0421*(Age*12)+1.9366) [3]	(0.004*Age^2+0.5348*Age+10.92) ± 3 [3]
	Female	(-2E-06*Age^3 + 0.0011*Age^2 - 0.1058*Age + 18.249)±(7E-09*Age^4 - 4E-06*Age^3 + 0.0009*Age^2 - 0.0579*Age + 2.2788) [3]	(-0.0204*Age^2 + 1.1067*Age + 7.7386) ± 3 [3]
Weight	**Male**	(-1E-07*(Age*12)^4+4E-05*(Age*12)^3-0.0052*(Age*12)^2+0.4118*(Age*12)+4.6681) ± (3E-10*(Age*12)^5-2E-07*(Age*12)^4+5E-05*(Age*12)^3-0.0051*(Age*12)^2+0.2379*(Age*12)-2.3971) [3]	(-0.0419*Age^3+1.684*Age^2-17.334*Age+78.678) ± 4.5 [3]
	Female	(-9E-09Age^4 - 6E-06Age^3 + 0.003Age^2 - 0.1028Age + 13.926) ± (4E-10Age5 - 3E-07Age4 + 5E-05Age3 - 0.0045Age2 + 0.1886Age - 1.4623) [3]	(-0.239*Age^2 + 9.6465*Age - 39.288) ± 4.5 [3]
BSA	**Both**	0.0235*((Height*100)^0.42246)*(Weight^0.51456) [4]	
Height	**Both**	sqrt(Weight/BMI)	

Table 2 a) Allometric equations describing organ and tissue weights for male children between 2-18 years

	2-7 years	7-18 years
Adipose	0.534*Weight-1.59*Age+3.03 ± 0.041 [11]	(1.51*BMI-0.7*Age-3.6*Sex+1.4)*Weight/100 ± 0.041 (Sex=0 for female, 1 for male) [12]
Blood	(-0.0623*(Age^5)+2.4425*(Age^4)-31.37*(Age^3) +149.98*(Age^2) +31.305*Age+393.7)/1000 ± 0.15 [13]	(3.33*BSA-0.81) ± 0.1 [12]
Bones	(-0.0306*(Age^5)+0.5222*(Age^4)+9.7109*(Age^3)-197.97*(Age^2)+1089.7*Age+546.6)/1000 ± 0.15 [13]	exp(0.0689+2.67*log(Height)) ± 0.166 [11]
Brain	(0.405*exp(-Age/629)*(3.68-2.68*exp(-Age/0.89)) ± 0.084 [12]	
Glands	(0.001*(Age^5)-0.0483*(Age^4)+0.8335*(Age^3)-6.6516*(Age^2)+27.512*Age+13.9 ± 0.015)/1000 [13]	
Gonads	(3.3+53*(1-abs(exp((-Age/17.5)^5.4)))/1000 ± exp(0.049) [12]	
Heart	(41.70+0.022*Age*365 ± 25)/1000 [14]	
Intestines	(-4.7817e-2*(Age^4)+1.925*(Age^3)-22.382*(Age^2)+107.09*Age+51.125)/1000 ± 0.05 [13]	
Kidneys	(35.29+0.015*Age*365+34.14+0.015*Age*365)/1000 ± 2.5 [14]	
Liver	(271.58+0.163*Age*365 ± 25)/1000 [14]	
Lungs	(41.31+0.039*Age*365+36.92+0.037*Age*365 ± 5)/1000 [14]	
Muscle	0.93*Weight-(Sum of organ weights) [12]	
Remaining	exp(-0.072+1.95*log(Height) ± 0.049) [12]	
Skin	exp(1.64*BSA-1.93) ± 0.049 [12]	(-0.0992*(Age^4)+4.2762*(Age^3)-62.165*(Age^2)+437.78*Age+203.2)/1000 ± 0.2*(-0.0992*(Age^4)+4.2762*(Age^3)-62.165*(Age^2)+437.78*Age+203.2)/1000 [15]
Spleen	(18.42+0.018*Age*365 ± 2.5)/1000 [14]	
Stomach	exp(-3.266+2.45*log(Height) ± 0.0965) [12]	
Thymus	(14*((7.1-6.1*exp(-Age/11.9))*((0.14+0.86*exp(-Age/10.3))))/1000 ± 0.049 [12]	

b) Allometric equations describing organ and tissue weights for female children between 2-18 years

	2-7 years	**7-18 years**
Adipose	0.642*Weight-0.12*Height-0.606*Age+8.98 ± 0.041 [11]	(1.51*BMI-0.7*Age+1.4)*Weight/100 ± 0.041 [12]
Blood	(0.0018*(Age^5)+0.0959*(Age^4)-4.4055*(Age^3)+ 44.442*(Age^2)+82.808*Age+292.26)/1000 ± 0.15 [13]	(2.66*BSA-0.46) ± 0.1 [12]
Bones	(-2.831e-3*(Age^5)-0.18184*(Age^4)+10.685*(Age^3)- 142.88*(Age^2)+782.05*Age+609.64)/1000 ± 0.15 [13]	exp(0.0689+2.67*log(Height)) ± 0.166 [11]
Brain	(0.373*exp(-Age/629)*(3.68-2.68*exp(-Age/0.89)) ± 0.084 [11]	
Glands	(0.001*(Age^5)-0.0483*(Age^4)+0.8335*(Age^3)-6.6516*(Age^2)+27.512*Age+13.9 ± 0.015)/1000 [13]	
Gonads	(3.3+90*(1-abs(exp((-Age/16.8)^6.7)))/1000 ± exp(0.049) [12]	
Heart	(41.70+0.022*Age*365 ± 25)/1000 [14]	
Intestines	(-0.0513*(Age^4)+2.0352*(Age^3)-23.478*(Age^2)+110.61*Age+49.229)/1000 ± 0.05 [13]	
Kidneys	(35.29+0.015*Age*365+34.14+0.015*Age*365)/1000 ± 2.5 [14]	
Liver	(271.58+0.163*Age*365 ± 25)/1000 [14]	
Lungs	(41.31+0.039*Age*365+36.92+0.037*Age*365 ± 5)/1000 [14]	
Muscle	0.93*Weight-(Sum of organ weights) [12]	
Remaining	exp(-0.072+1.95*log(Height) ± 0.049) [12]	
Skin	exp(1.64*BSA-1.93) ± 0.049 [12]	(0.00476622*(Age^5)-0.27924*(Age^4)+6.3444*(Age^3)- 70.113*(Age^2)+429.85*Age+252.06)/1000 ± 0.20*(0.00476622*(Age^5)- 0.27924*(Age^4)+6.3444*(Age^3)-70.113*(Age^2)+429.85*Age+252.06)/1000 [15]
Spleen	(18.42+0.018*Age*365 ± 2.5)/1000 [14]	
Stomach	exp(-3.266+2.45*log(Height) ± 0.0965) [12]	
Thymus	(14*((7.1-6.1*exp(-Age/11.9))*((0.14+0.86*exp(-Age/10.3))))/1000 ± 0.049 [12]	

Table 3 Equations for cardiac output and percentages of blood flow rate to each organ from the cardiac output adjusted according to literature data [6]

	2-7 years		**7-18 years**	
Cardiac output	60*(10^(0.8914*$\log_{10}$(Weight)-0.654)) [16]		(3.107+(0.012*Weight^1.369))*60 [17]	
Gender → Organ/Tissue ↓	Male	Female	Male	Female
Adipose	0.04	0.05	0.04	0.06
Bone	0.02	0.02	0.04	0.04
Brain	0.38	0.38	0.24	0.24
Gut (Q_{gu})	0.12	0.13	0.14	0.15
Hepatic artery	0.08	0.08	0.06	0.07
Kidneys	0.13	0.11	0.17	0.13
Lungs	0.02	0.02	0.02	0.02
Muscle	0.05	0.06	0.12	0.11
Portal vein (Q_{pv})	$Q_{gu}+Q_{st}+Q_{sp}$			
Remaining	0.07	0.06	0.08	0.08
Skin	0.03	0.03	0.04	0.04
Spleen + Pancreas (Q_{sp})	0.05	0.05	0.04	0.04
Stomach (Q_{st})	0.01	0.01	0.01	0.01

Table 4 Physicochemical properties, *in vitro* and population pharmacokinetic data of lorazepam and ceforanide

	Lorazepam	**Ceforanide**
Molecular weight	321	519
log $P_{o:w}$	2.39 [9]	-3.7 [18]
Protein binding (%)	0.93 [19]	80.6 [18]
pK_a	1.3 (base), 11.5 (acid) [9]	2.55 (acid), 9.14 (base) [18]
R	0.642 [9]	†0.1173
UGT2B7 CL_{int}	0.439 [9]	-
Renal clearance	0.01 [9]	-
Plasma clearance	-	72 ± 21 [2]

log $P_{o:w}$ – Partition coefficient between octanol and water; pKa – logarithmic value of the dissociation constant; R – blood-to-plasma drug ratio; CL_{int} – intrinsic clearance; UGT - uridine diphosphate glucuronosyltransferase (ml/min/g of liver), renal clearance is in ml/min/kg, plasma clearance is expressed in ml/min · 1.73 m^2; † the value was computed from the correlation provided by Paixão et al. [20]

2. Results

The mean simulated values of the anatomy and blood flow rates of children and adolescents were compared against literature values [5, 6]. The validation was performed for ages 2, 5, 10 and 15 years [6]. The simulated paediatric characteristic values for BSA, height and weight are in agreement with literature data as shown in Table 5. Allometric equations from various literature sources describing the organ and tissues weights and blood flow rates of children and adolescents are in agreement with the published data, shown in Table 6 and Table 7. A separate 'remaining' compartment was created to accommodate the unaccounted weight (data not shown) and blood flow rate in order to improve the model prediction. Allometric equations for 2 years were assumed to predict anatomy and physiology between the ages 2 and 5 with relative accuracy and precision. Observed growth pattern was slightly different from 7 years onwards due to which different equations were used for allometric scaling [3]. Due to large variation in anatomical and physiological characteristics among children and adolescents, broader validation range i.e. ± 100% was assumed. The mean values from the chosen allometric equations were between the assumed ranges from the reported literature values except for the lung weight of a 10-year-old child (101.2 %). The mean simulated blood flow rates were ± 50% from the literature value for all the age groups (Table 7).

. The pharmacokinetics were predicted across all age groups from 3-17 years and the mean value was compared with clinical data. Simulated lorazepam and ceforanide pharmacokinetics were compared against clinical data as shown in Table 8. For lorazepam, the C_{max}, AUC and V_d were +37.5 %, +22.2 % and -14.6 % from clinical values [1]. Validation of intramuscular ceforanide against clinical data had a deviation of +7.4 %, +16.6 % and -8.1 % for C_{max}, AUC and V_d respectively [2]. The simulated C_{max} and AUC values are slightly high which can be explained by the low volume of distribution observed. Due to unavailability of data, the blood-to-plasma ratio, fraction unbound, intrinsic and renal clearance were not altered across age groups.

Table 5 Validation of characteristic features against literature data for different ages (data represented as Male/Female) [5, 6]

Years →	**2**		**5**		**10**		**15**	
Characteristic ↓	**Simulated**	**Reference**	**Simulated**	**Reference**	**Simulated**	**Reference**	**Simulated**	**Reference**
BSA	0.76/0.74	NA	0.91/0.91	0.78/0.78	1.20/1.14	1.12/1.12	1.67/1.49	1.62/1.55
Height	0.87/0.87	NA	1.09/1.09	1.09/1.09	1.39/1.37	1.38/1.38	1.80/1.53	1.67/1.61
Weight	12.7/12.1	12.6/11.9	18.0/17.2	18.7/17.7	31.0/34.0	31.4/32.6	56.0/52.0	56.7/53.7

Table 6 Validation of organ weights (kg) against literature data for different ages (Data represented as Male/Female) [5, 6]

Years →	**2**		**5**		**10**		**15**	
Organs ↓	**Simulated**	**Reference**	**Simulated**	**Reference**	**Simulated**	**Reference**	**Simulated**	**Reference**
Adipose	3.17/2.91	3.76/3.72	4.68/4.26	5.50/5.50	7.45/9.28	8.60/8.60	11.6/14.2	12.0/18.7
Bones	0.74/0.74	0.85/0.82	2.49/2.49	2.43/2.43	4.6/4.47	4.50/4.50	8.32/8.32	7.18/7.18
Brain	1.50/1.50	1.12/1.03	1.48/1.36	1.31/1.31	1.47/1.48	1.40/1.40	1.46/1.34	1.30/1.30
Glands	0.02/0.02	0/0	0.06/0.06	0.04/0.04	0.07/0.07	0.06/0.06	0.06/0.06	0.10/0.10
Heart	0.07/0.06	0.07/0.06	0.08/0.08	0.09/0.09	0.12/0.12	0.14/0.14	0.16/0.16	0.22/0.22
Intestines	0.20/0.19	0.19/0.19	0.24/0.24	0.34/0.34	0.33/0.33	0.58/0.58	0.70/0.69	0.82/0.82
Kidneys	0.10/0.10	0.09/0.08	0.12/0.12	0.11/0.11	0.18/0.18	0.18/0.18	0.23/0.23	0.24/0.24
Liver	0.46/0.45	0.48/0.46	0.57/0.57	0.57/0.57	0.87/0.87	0.83/0.83	1.16/1.16	1.30/1.30
Lungs	0.18/0.18	0.24/0.24	0.22/0.22	0.13/0.13	0.38/0.38	0.21/0.21	0.52/0.52	0.29/0.29
Muscle	3.37/2.92	2.83/2.83	5.23/4.67	5.60/5.60	7.90/10.42	11.0/1.01	17.5/14.6	17.0/17.0
Skin	0.52/0.49	0.41/0.39	0.64/0.62	0.57/0.57	1.65/1.65	0.82/0.82	2.19/2.19	1.70/1.70
Spleen	0.04/0.04	0.07/0.07	0.05/0.05	0.05/0.05	0.08/0.08	0.08/0.08	0.12/0.12	0.13/0.13
Stomach	0.03/0.03	0.03/0.03	0.05/0.05	0.05/0.05	0.09/0.09	0.09/0.09	0.16/0.11	0.12/0.12
Thymus	0.02/0.02	NA	0.03/0.03	0.03/0.03	0.03/0.03	0.04/0.04	0.03/0.03	0.03/0.03

Table 7 Validation of organ blood flows (L/h) for different ages against literature values (Data represented as Male/Female) [6]

Years →	**2**		**5**		**10**		**15**	
Organs ↓	**Simulated**	**Reference**	**Simulated**	**Reference**	**Simulated**	**Reference**	**Simulated**	**Reference**
Cardiac Output	129/122	124/114	176.5/132.7	172.8/157.8	269.5/272.5	234/224.4	363.9/347.2	346.2/309
Adipose	5.1/4.8	5.4/5.8	7.1/8	7.2/7.8	10.8/16.4	10.8/14	14.5/20.8	13.7/25
Brain	41.0/38.7	54.4/50.1	63.2/32	62.7/57.8	65.6/65.8	55.5/51	46.6/42.6	45/39.9
Gut	11.3/10.7	13.1/12.4	24.7/19.9	23.5/22.2	37.7/40.9	35.5/35.5	50.9/52	49.7/47.7
Hepatic Artery	32.1/31.0	43.2/40.8	10.6/9.3	11.3/10.6	16.2/19.1	14.6/15	21.8/24.3	22.7/21.5
Kidney	11.9/11.3	18.5/13.3	30/17.2	22.6/16.7	45.8/35.5	42.6/30	61.8/45.1	63.2/46.8
Lungs	8.4/8.0	9.2/8.28	3.5/2.7	3.3/3.1	5.4/5.5	4.1/4.8	7.3/6.9	8.6/7.2
Muscle	1.6/1.5	2.3/2.3	13.5/14.5	13.1/13.1	31.4/29.8	25.7/25.7	57/45.8	56.2/39.8
Remaining	5.1/4.8	4.9/4.9	14.1/10.6	11/7.3	21.6/21.8	17.7/18.4	29.1/27.7	37/35
Skin	3.4/3.2	3.9/3.7	7.1/5.3	5.3/5.1	10.8/10.9	7.7/7.8	14.5/13.9	14.5/12
Spleen	2.6/2.4	5.0/4.6	7.1/5.3	6.4/6	10.8/10.9	8.9/9.5	14.5/13.9	15.4/13.8
Stomach	1.2/1.1	1.2/1.1	1.8/1.3	2/1.8	2.7/2.7	3.2/3	3.6/3.5	5/4.5

Table 8 Validation of lorazepam [1] and ceforanide [2] paediatric model against clinical data

Lorazepam			
	C_{max} (ng/ml)	**AUC** (ng.h/ml)	**V_d** (L/kg)
Simulated	77.14 ± 15.82	1005.62 ± 268.48	1.64 ± 0.13
Clinical	56.1 ± 44.9	822.5 ± 706.1	1.92 ± 0.84
Ceforanide			
	C_{max} (µg/ml)	**AUC** (µg.h/ml)	**V_d** (L/kg)
Simulated	60.4 ± 14.4	250 ± 74.0	0.24 ± 0.16
Clinical	56.3 ± 14.0	215 ± 61.0	0.26 ± 0.67

References

1. Chamberlain, J.M., et al., *Pharmacokinetics of Intravenous Lorazepam in Pediatric Patients with and without Status Epilepticus.* The Journal of Pediatrics, 2012. **160**(4): p. 667-672.e2.
2. Dajani, A.S., et al., *Pharmacokinetics of intramuscular ceforanide in infants, children, and adolescents.* Antimicrobial Agents and Chemotherapy, 1982. **21**(2): p. 282-287.
3. Centers for Disease Control and Prevention, *CDC growth charts: United States*, in *National Center for Health Statistics*. 2000.
4. Gehan, E.A. and S.L. George, *Estimation of human body surface area from height and weight.* Cancer Chemotherapy Reports Part 1, 1970. **54**(4): p. 225-&.
5. Valentin, J., *Annals of the ICRP: Basic Anatomical and Physiological Data for Use in Radiological Protection: Reference Values*. 2003, The International Commission on Radiological Protection.
6. Bjorkman, S., *Prediction of drug disposition in infants and children by means of physiologically based pharmacokinetic (PBPK) modelling: theophylline and midazolam as model drugs.* Br J Clin Pharmacol, 2005. **59**(6): p. 691-704.
7. Rajoli, R.K.R., et al., *Physiologically Based Pharmacokinetic Modelling to Inform Development of Intramuscular Long-Acting Nanoformulations for HIV.* Clinical Pharmacokinetics, 2014. **54**(6): p. 639-650.
8. Peters, S., *Evaluation of a Generic Physiologically Based Pharmacokinetic Model for Lineshape Analysis.* Clinical Pharmacokinetics, 2008. **47**(4): p. 261-275.
9. Maharaj, A.R., J.S. Barrett, and A.N. Edginton, *A Workflow Example of PBPK Modeling to Support Pediatric Research and Development: Case Study with Lorazepam.* AAPS J, 2013. **15**(2): p. 455-64.
10. Poulin, P. and F.P. Theil, *Prediction of pharmacokinetics prior to in vivo studies. 1. Mechanism-based prediction of volume of distribution.* J Pharm Sci, 2002. **91**(1): p. 129-56.
11. Price, P.S., et al., *Modeling Interindividual Variation in Physiological Factors Used in PBPK Models of Humans.* Critical Reviews in Toxicology, 2003. **33**(5): p. 469-503.
12. Bosgra, S., et al., *An improved model to predict physiologically based model parameters and their inter-individual variability from anthropometry.* Crit. Rev. Toxicol., 2012. **42**(9): p. 751-767.
13. Haddad, S., C. Restieri, and K. Krishnan, *Characterization of age-related changes in body weight and organ weights from birth to adolescence in humans.* Journal of Toxicology and Environmental Health-Part A, 2001. **64**(6): p. 453-464.
14. Shankle, W.R., B.H. Landing, and J. Gregg, *Normal organ weights of infants and children: graphs of values by age, with confidence intervals.* Pediatric pathology / affiliated with the International Paediatric Pathology Association, 1983. **1**(4): p. 399-408.
15. McQueen, C.A., et al., *Comprehensive Toxicology, Volumes 1-14 (2nd Edition)*. Elsevier.
16. Ginsberg, G., et al., *Physiologically Based Pharmacokinetic (PBPK) Modeling of Caffeine and Theophylline in Neonates and Adults: Implications for Assessing Children's Risks from Environmental Agents.* Journal of Toxicology and Environmental Health, Part A, 2004. **67**(4): p. 297-329.
17. Williams, L.R., *Reference values for total blood volume and cardiac output in humans*. 1994.
18. DrugBank. *Ceforanide*. 2017 [cited 2017 06/03/2017]; Available from: https://www.drugbank.ca/drugs/DB00923.
19. DrugBank. *Lorazepam*. 2013 [cited 2016 13/5/2016]; Available from: http://www.drugbank.ca/drugs/DB00186.
20. Paixão, P., L.F. Gouveia, and J.A.G. Morais, *Prediction of drug distribution within blood.* European Journal of Pharmaceutical Sciences, 2009. **36**(4–5): p. 544-554.

The NIHMS has received the file '40262_2017_557_MOESM1_ESM.pdf' as supplementary data. The file will not appear in this PDF Receipt, but it will be linked to the web version of your manuscript.